Jurnal Teknologi

Full Paper

# EXPERIMENTAL STUDY ON NONLINEAR SHEAR STRENGTH BEHAVIOR OF A TROPICAL GRANITIC RESIDUAL SOIL (GRADE VI) AT VARIOUS INITIAL MOISTURE CONTENTS

Pooya Saffari[a], Mohd Jamaludin Md Noor[a*], Shervin Motamedi[b], Roslan Hashim[b], Zubaidah Ismail[b], Basharudin Abdul Hadi[a]

[a]Faculty of Civil Engineering, University Technology MARA, 40450, Shah Alam, Malaysia
[b]Department of Civil Engineering, Faculty of Engineering, University of Malaya, 50603, Kuala Lumpur, Malaysia

**Article history**
Received
*10 June 2016*
Received in revised form
*14 December 2016*
Accepted
*10 January 2017*

*Corresponding author
2011807408@isiswa.uitm.edu.my

## Graphical abstract

## Abstract

The conventional theories of soil mechanics use linear envelope to derive shear strength; this however, leads to an overestimation of the factor of safety in the examination of slopes. Therefore, the incorporation of methods that acknowledge the existence of non-linear characteristics of shear strength is necessary in the analysis of slopes specifically. This is due to the substantial influence of non-linear shear strength behavior on the slope failure mechanism when they are at low stress levels. In this paper, the nonlinearity of shear strength for grade VI granitic residual soil is studied. "Non-Axis Translation Consolidated Drained Triaxial" tests were performed at various ranges of net stress and suction. Thereafter, to characterize shear strength behavior, shear strength parameters were derived. The soil-water characteristic curve was plotted after conducting "Pressure Plate Extractor" test at a series of suction. The result substantiated the non-linearity of shear strength for granitic residual soil based on net stress and suction.

*Keywords*: Net stress, suction, unsaturated soil, shear strength, triaxial test

## Abstrak

Teori-teori kovensional mekanik tanah mengaplikasikan model hamparan bergaris lurus (liner) untuk mengambarkan kekuatan daya ricih sesuatu jenis tanah. Bagaimanapun, model ini sentiasa menunjukan keputusan tidak tepat apabila didapati terlebih menganggar aspek keselamatan kestabilan sesenuah cerun semasa pemeriksaan dijalankan. Walaubagaimanapun, dengan pengenalan kepada model hamparan bergaris melengkung dalam menganalisa sesuatu cerun secara terperinci didapati lebih tepat keputusannya. Perkara ini berkaitan pengaruh yang kuat model ini mengaplikasikan kelakuan sebenar kekuatan ricihan tanah bagi menganalisa mekanisma keruntuhan sesuatu cerun terutamanya di zon tekanan rendah. Kajian ini telah dijalankan menggunakan tanah berbaki gred VI dan mengaplikasikan model hamparan melengkung. Eksperimen - eksperimen menggunakan teknik, 'Non-Axis Translation Consolidated Drained Triaxial' telah dijalankan di pelbagai julat tekanan dan sedutan sebenar.Seterusnya, adalah untuk mengspesifikasikan kelakuan berperimeter kekuatan ricih telah diperincikan. Kemudian, untuk memodelkan kelakuan melengkung tanah-air telah diplotkan selepas ujian - ujian bersiri sedutan dikenali 'pressure plate extractor' dijalankan. Semua hasil keputusan ujian didapati mengikut model hamparan melengkung bagi kekuatan ricih tanah untuk tanah jenis berbaki dan ianya berkadaran dengan tekanan dan sedutan sebenar tanah di lokasi se.

*Kata kunci*: tekanan bersih, sedutan, tanah tak tepu, kekuatan ricih, ujian tiga paksi

## 1.0 INTRODUCTION

The concept of shear strength is widely applicable in geotechnical projects such as the stability of slopes, lateral earth pressure as well as bearing capacity. The capability of a soil to resist shear loads defines a soil's shear strength and such a shear strength depends on two stress state variables; suction and net stress.

Conventional theories describe shear strength as based on Mohr-Coulomb failure envelope [1](See Equation 1). The linear correlation between shear strength, $\tau$, and effective stress, $(\sigma-u_w)$, is defined in Equation 1 below. Although the shear strength of saturated soils can be considerably estimated by employing the equation; it fails to define the true shear strength behavior of partially saturated soils [2]. $\tau$ is the shear strength, c' is the cohesion intercept, $\sigma$ is the total stress, $u_w$ is the pore-water pressure and $\emptyset'$ is the internal friction angle in Equation 1 below, .

$$\tau = c' + (\sigma - u_w)\tan\emptyset' \quad (1)$$

In a partially saturated condition, the attraction force induced from the water meniscus surface tension makes the soil structure stronger. Such an attraction force is known as suction, $(u_a-u_w)$, and has significant influence on shear strength behavior. Therefore, any shear strength model for partially saturated soil condition must incorporate both suction and net stress. The first linear equation which describes the shear strength of unsaturated and partially saturated soils by extending the Mohr-Coulomb failure envelope was introduced by Fredlund *et al.*, (1978) [3] (See Equation 2). The authors considered net stress, $(\sigma-u_a)$, and suction, $(u_a-u_w)$, as two stress state parameters of the soil in partially saturated condition. $u_a$ is the air pressure, $\emptyset^b$ is the angle of the line in matric suction versus stress graph when net stress is constant, as shown in Equation 2 below.

$$\tau = c' + (\sigma - u_a)\tan\emptyset' + (u_a - u_w)\tan\emptyset^b \quad (2)$$

The linear behavior for shear strength in a partially saturated soil was claimed by Fredlund *et al.*, (1978) [3]. However, it is observed that there are indications that there is a rapid decline in shear strength to the point of zero where net stress approaches zero; for gravels by Charles and Watts (1980) [4], clays by Bishop (1966) [5], and sands by Fukushima and Tatsuoka (1984) [6]. In addition, Indraratna *et al.*, (1993) [7]; Rahardjo *et al.*, (1995) [8] and Md.Noor *et al.*, (2008) [9] reported similar non-linearity in shear strength behavior with respect to net stresses. Hence, it can be claimed that shear strength is not linear with respect to net stress [3].

A soil's moisture content when decreased, leads to an increase in suction [3]. The authors also believed that as suction increases, shear strength also amplifies. However, where suction grows beyond the residual suction, it is observed that there are evidences of shear strength decreases [10]. Besides, Escario and Saez (1986) [11]; Rassam and Williams (1999) [12]; Toll *et al.*, (2000) [13] reported that the shear strength suddenly drops as suction approached zero. Therefore, the assumption of the absolute linear relativity of shear strength pertaining to suction is not always true.

The main cause of shallow slope failure in tropical countries is directly linked with the non-linearity of the shear strength based on suction and net stress [14]. Generally, shallow slope failure occurs above the ground water level and within the partially saturated zone. In addition, the depth of a shallow slope failure is normally less than 5 m [14]. Therefore, the net stress that caused the failure is relatively low (<100 kPa). Once rain infiltrates the ground, the soil then becomes wet and shear strength decreases. Consequently, the slope becomes unstable [14, 15].

The conventional theories of soil mechanics use linear envelope to derive shear strength; this however leads to an overestimation of the factor of safety in the slope analysis. In addition, back analysis of slope failure using conventional methods often fail to achieve a factor of safety of less than unity [16]. Therefore, the application of a modified shear strength concept to comprehend the true shear strength behavior of soil is important. The model used must characterize the non-linearity of shear strength with regards to net stress as well as suction.

Recently, in relation to the prediction of the shear strength of unsaturated soils, several shear strength models were introduced [10, 17-20]. [10] developed an equation by the study on behaviour of various sands and gravel due to effective stress and suction. They observed that majority of tested soils behave linearly at high stress levels, however, they exhibit the non-linear behaviour at low stress levels. As a result, they introduced "Curved-Surface Envelope Extended Mohr Coulomb Shear Strength Model" (CSE Model) which represents the curvilinear behavior of shear strength in saturated and unsaturated conditions. The model is a development of Mohr-Coulomb circles and defined based on geometric parameters, i.e. parameters represent geometric determination instead of using fitting parameters. The authors claimed that when the model is applied on unsaturated soils, the true non-linearity of shear strength behavior in relation to suction as well as net stress can be simulated. Equations (3) and (4) are used to best fit saturated shear strength of residual soil, whereas Equations (5) and (6) are used to best fit the unsaturated shear strength of residual soil. The derivations of Equations (3) to (6) were explained in detail in [10], and they are not repeated in this paper.

$$\tau_f = \frac{(\sigma-u_w)}{(\sigma-u_w)_t}\left(1 + \frac{(\sigma-u_w)_t-(\sigma-u_w)}{N\,(\sigma-u_w)_t}\right)\tau_t \quad (3)$$

$$\tau_f = (\sigma - u_w)\tan\emptyset'_{minf} + (\tau_t - (\sigma - u_w)_t\tan\emptyset'_{minf}) \quad (4)$$

$$c_{s=}\frac{(u_a-u_w)}{(u_a-u_w)_r}\left[1+\frac{(u_a-u_w)_r-(u_a-u_w)}{(u_a-u_w)_r}\right]c_s^{max} \quad (5)$$

$$c_s = c_s^{max}\left(\frac{(u_a-u_w)_u-(u_a-u_w)}{(u_a-u_w)_u-(u_a-u_w)_r}\right)\times\left(1-\frac{(u_a-u_w)_r-(u_a-u_w)}{(u_a-u_w)_u-(u_a-u_w)_r}\right)\tau_t \quad (6)$$

Where $\tau_f$ is shear strength at saturation; $c_s$ is apparent shear strength due to suction; $\emptyset'_{min\ f}$ is the lowest friction angle when failure occurs; $\tau_t$ is the transition shear strength; $(\sigma\text{-}u_w)_t$ is the transition effective stress; $(u_a\text{-}u_w)_r$ is the residual suction; $(u_a\text{-}u_w)_u$ is the ultimate suction when net stress is equivalent to zero; $c_s^{max}$ is the maximum apparent cohesion; and N is the variable which can be calculated from Equation 7.

$$N=\frac{1}{1-((\sigma-u_w)\frac{\tan\emptyset'_{min\,f}}{\tau_t}}} \quad (7)$$

The model was validated by the data reported by Gan and Fredlund (1996) [21], Toll *et al.*, (2000) [13] and also the data collected from consolidated drained triaxial test on Limestone gravel. However, it is important to evaluate the compliance of the model for those soils which are frequently involved in slope failures and shallow landslides, specifically.

This paper aims to substantiate the non-linear shear strength behavior of tropical granitic residual soil based on the CSE Model. It helps to unveil the mechanical behavior of this type of soil which is frequently a part of shallow slope failure in the tropics. Besides that, shear strength plays the fundamental role in the slope failure. Hence, the investigation of shear strength within the stress level of the shallow landslide is essential. Shear strength variables are verified and the non-linear shear strength behavior of Granitic residual soil (grade VI) relative to net stress and suction is characterized at a wide range of suction and net stresses independently. In addition, the validation of the CSE Model providing the description of shear strength behavior of partially saturated soils is evaluated.

## 2.0 METHODOLOGY

### 2.1 Soil Sampling and Characteristics of the Soil Tested

The soil tested in this study was granitic residual soil (grade VI). The samples were taken from Rawang, Selangor, Malaysia. The specimens were reddish brown and were air-dried for a week in normal laboratory temperature (25 °C). Further, a rubber hammer was used to break down the soil lumps. All soil specimens used had the same initial dry unit weight (13.6 kN/m$^3$). According to the Standard Test Method for Particle-Size Analysis of Soils (ASTM D422), the specimen constituted dominantly of very silty gravely sand. Table 1 provides an overview of the characteristics of the soil sample.

**Table 1** The basic properties of the soil sample

| Basic Properties | Particles Size Distribution | | | | Attemberg Limit | | | Dry Unit Weight (KN/m$^3$) | Spacefic Gravity (Mg/m$^3$) |
|---|---|---|---|---|---|---|---|---|---|
| | Clay % | Silt% | Sand % | Gravel % | PL% | LL % | PI % | | |
| **Tested Soil (granitic residual soil)** | 8.59 | 20.7 | 48.8 | 21.9 | 23 | 30 | 7 | 13.6 | 2.57 |

### 2.2 Testing Methods

In this study, two sets of equipment were used: (a) equipment the application of the Triaxial Multistage Compression test for saturated and unsaturated soil specimens and (b) equipment for the application of the Pressure Plate Extractor test.

#### *2.2.1 Non-Axis Translation Multistage Consolidated Drained Triaxial Test*

The Non-Axis Translation Multistage Consolidated Drained Triaxial test (CD) was conducted to define the shear strength variable of granitic residual soil on saturated and unsaturated specimens. The tests were conducted in accordance with the Standard Test Method for Consolidated Undrained Triaxial Compression Test for Cohesive Soils (ASTM D4767). In addition, the stress-strain response of the soil samples in various ranges of suction and stresses were characterized. The Multistage Triaxial test provides more than one stress state at the point of failure for each specimen. The procedure time is reduced here because of the time saved during the stages of the preparation of specimen and its saturation.

Here, the stages of the preparation of specimen and its saturation are comparable to ordinary triaxial methods. The differentiation is obvious only during the shearing stage. To put this simply, here, the specimen is loaded. The threshold is reached when the stress approaches to the maximum amount of stress before failure. The threshold can be specified by the stress-

strain curve during shearing. Thereafter, the specimen is unloaded to zero stress. After that, the specimen is loaded again after the confining pressure ($\sigma_3$) is increased to a new desired value. At the final stage, shearing is continued until the specimen fails.

For the purposes of this paper, the Multistage Consolidated Drained Triaxial test was applied to specimens that are in saturated and unsaturated condition. Four different isotropic confining pressures were applied (50, 100, 200 and 300 kPa). At 3%, 6%, 9% and 12% initial moisture content (14.01%, 14.42%, 14.82%, 15.23% degree of saturation respectively), the partially saturated specimens were tested. The identical dry unit weight (13.6 kN/m3) and volume (100 mm height and 50 mm diameter) were used for each specimen to generate homogenous specimens.

The testing method for partially saturated specimens was similar to the method used by Bishop and Blight (1963) [5]. In the test of the unsaturated specimens, the back pressure line was released to the atmosphere and the pore-water was drained. As a result, air pressure equivalent to zero (atmospheric air pressure), suction within specimens only existed from the negative microscopic water meniscus between the soil particles and was kept constant during the shearing stage. It was controlled by measuring the moisture content of the specimen after the test. It was observed that there was a negligible difference between the moisture content of specimens before and after the triaxial test. The value of suction related to each moisture content was obtained from the Soil Water Characteristic Curve (Section 2.2.2). The arrangement of triaxial apparatus for the CD Triaxial test on the partially saturated specimens is shown in Figure 1.

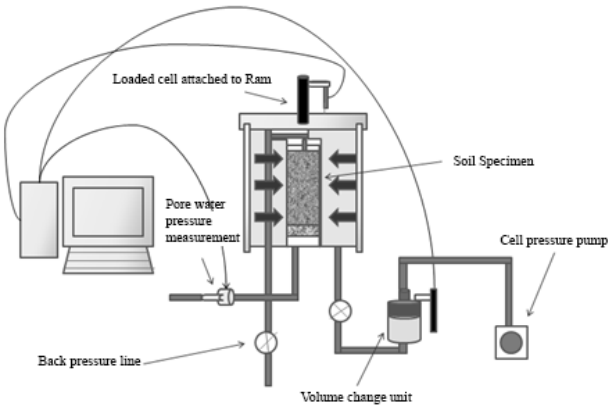


**Figure 1** Arrangement of CD Triaxial apparatus on partially saturated specimens

### 2.2.2 *Pressure Plate Extractor Apparatus*

In order for the soil-moisture characteristic curve to be found and for the residual soil to be defined and determined, the Pressure Plate Extractor test was performed. This test was performed in accordance with the procedure described in the Standard Test Methods for Determination of the Soil Water Characteristic Curve for Desorption Using a Hanging Column, Pressure Extractor, Chilled Mirror Hygrometer, and/or Centrifuge (ASTM D6836).

The Pressure Plate apparatus is made up of two core parts, which are: (a) an air pressure chamber and (b) a high-air entry ceramic disc. At each stage, three soil samples were placed on circular rings (50 mm diameter and 10 mm height). Then, they were mounted on the high-air entry ceramic disc. 13.6 kN/m3 with the same initial moisture content of 15% was defined as the dry unit weight for all soil specimens and all specimens were compacted in the same dry unit weight to assure the gain of homogeneity for the samples. The rings envelop soil specimens and were placed into the chamber and on the ceramic disc. Further, the samples were soaked with water. Thereafter, the application of the chosen air pressure was done to all soil samples. Due to the fact that the chamber's bottom (the part which is under the high-air entry disc) was joined to atmospheric pressure, the water pressure was equivalent to zero. Hence, it can be seen that the air pressure that was applied and the matric suction is equivalent [22]. The moisture content of the specimens was recorded at the end of the test. This experiment was conducted for a range of matric suction from 10 kPa to 900 kPa. The matric suction was applied in 10 kPa intervals for up to 100 kPa and beyond that, the pressure was applied in interval of 50 kPa. Figure 2 shows the schematic view of Pressure Plate Extractor apparatus.

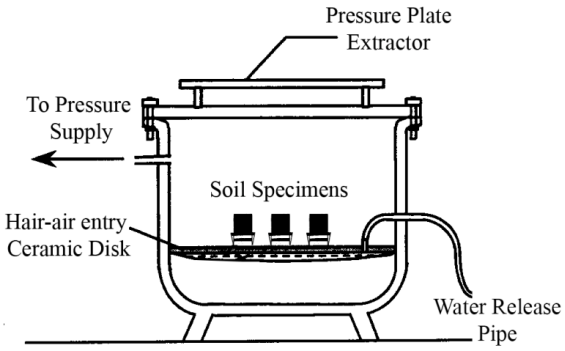


**Figure 2** Schematic view of Pressure Plate Extractor apparatus

## 3.0 RESULTS AND DISCUSSION

### 3.1 Soil Water Characteristic Curve (SWCC)

The SWCC curve was plotted based on gravimetric moisture content for three tested specimens (series 1, series 2, series 3) where residual suction is at 220 kPa and the residual gravimetric moisture content is 8%

(Figure 3). It is observed that the curve shape and value of residual suction matched perfectly when a comparison is done between the soil-water characteristic curve for the tested soil (highly silty sand) and the given typical soil-water characteristic curves [23]. Besides that, the matric suction linked to each specimen from SWCC can be acquired and then use in the Curved-Surface envelope. The value of matric suctions derived from SWCC for unsaturated condition in the proposed moisture contents (3, 6, 9 and 12 %) are presented in Table 2. For example, for 6 % moisture content, the matric suction is equal to 580 kPa.

**Table 2** Value of matric suction related to unsaturated specimens from SWCC

| Water content (%) | Suction (kPa) |
|---|---|
| **12** | 120 |
| **9** | 200 |
| **6** | 580 |
| **3** | 1500 |

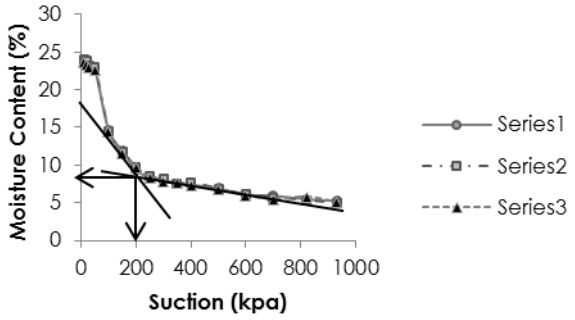


**Figure 3** SWCC curve based on gravimetric moisture content

## 3.2 Multistage CD Triaxial Test

The maximum deviator stress, $q_{max}$, in various ranges of effective stress for both the unsaturated and saturated specimen was obtained based on Non-Axis Translation Multistage Consolidated Drained triaxial test. Figure 4 provides the maximum deviator stress under various net stresses for each specimen. It shows that the maximum deviator stress is reduced from unsaturated specimen to saturated specimens for each specimen in the same effective stress. For example, for the effective stress of 50 kPa, the maximum deviator stress decreased from 135 kPa (12 % moisture content and 120 kPa suction) to 82 kPa (in a fully saturated condition and zero suction). Interestingly, when the moisture content increases (suction decreases) from 3 % to 6 % (suction from 1500 kPa to 580 kPa), the maximum deviator stress was elevated. For example, for the effective stress of 100 kPa, the maximum deviator stress increased from 333 kPa (3 % moisture content) to 390 kPa (6 % moisture content). The highest deviator stress in unsaturated condition occurred at 6 % moisture content.

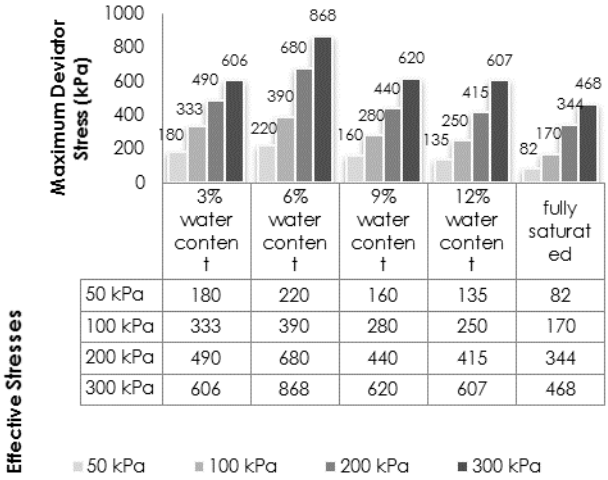


**Figure 4** Maximum deviator stress under various net stresses for each specimen

Adversely, the value of maximum deviator stress in the same effective stress range decreased when the moisture content increases (suction decrease) beyond the 6 % moisture content. For example, for 200 kPa of effective stress, the value of maximum deviator stress decreased from 680 kPa (6 % moisture content) to 440 kPa (9 % moisture content).

In order to determine Mohr Coulomb circles for each specimen, the minor effective stresses, $\sigma'_3$, and major effective stresses, $\sigma'_1$, were obtained from Figure 4. Thereafter, curvi-linear shear strength envelopes were drawn based on these Mohr circles in accordance with CSE model using Equations 3 and 4. Minimum friction angle at failure, $\emptyset'_{min\ f}$, apparent shear strength, c ', transition effective stress, $(\sigma - u_w)_t$, and transition shear strength, $\tau_t$ were procured. For example, in fully saturated condition and for targetted effective stress of 50 kPa, the applied cell pressure was 295 kPa. The pore pressure and maximum deviator stress while failure, were recorded at 257 kPa and 82 kPa, respectively. The minor effective stress was calculated from the difference between cell pressure and pore water pressure (38 kPa). Finally, the major effective stress was obtained from the summation of minor effective stress and maximum deviator stress (120 kPa). Table 3, summarizes the data obtained from multistage consolidated drained triaxial test in saturated and unsaturated conditions.

**Table 3** Summery of data obtained from multistage consolidated drained triaxial test

| Soil specimen description | Targeted effective stress (kPa) | Cell pressure (kPa) | Pore water pressure (kPa) | Maximum deviator stress, q (kPa) | minor effective stresses, $\sigma'_3$ (kPa) | major effective stresses, $\sigma'_1$ (kPa) |
|---|---|---|---|---|---|---|
| **3% water content** | 50 | 50 | 0 | 180 | 50 | 230 |
| | 100 | 100 | 0 | 333 | 100 | 433 |
| | 200 | 200 | 0 | 490 | 200 | 690 |
| | 300 | 300 | 0 | 606 | 300 | 907 |
| **6% water content** | 50 | 50 | 0 | 220 | 50 | 270 |
| | 100 | 100 | 0 | 390 | 100 | 490 |
| | 200 | 200 | 0 | 680 | 200 | 880 |
| | 300 | 300 | 0 | 867 | 300 | 1168 |
| **9% water content** | 50 | 50 | 0 | 160 | 50 | 210 |
| | 100 | 100 | 0 | 280 | 100 | 380 |
| | 200 | 200 | 0 | 440 | 200 | 640 |
| | 300 | 300 | 0 | 620 | 300 | 920 |
| **12% water content** | 50 | 50 | 0 | 135 | 50 | 185 |
| | 100 | 100 | 0 | 250 | 100 | 350 |
| | 200 | 200 | 0 | 415 | 200 | 615 |
| | 300 | 300 | 0 | 607 | 300 | 907 |
| **Fully saturated** | 50 | 295 | 257 | 82 | 38 | 120 |
| | 100 | 345 | 265 | 170 | 80 | 250 |
| | 200 | 445 | 270 | 344 | 175 | 519 |
| | 300 | 545 | 274 | 468 | 271 | 739 |

Figure 5, illustrates Mohr circles and curvi-linear shear strength envelope for the specimen in fully saturated condition. As it can be observed, when effective stress approaches zero, non-linear behavior of shear strength is illustrated at failure envelopes. Once the effective stress is low (<100 kPa), a steep drop in shear strength occurs. In additional, the linear shear strength envelope based on Terzaghi equation (Equation 2) was provided. From Figure 5, it is clearly obvious that linear shear strength envelope cannot perfectly cover Mohr circles at low stress levels (less than 100 kPa) and governs a overestimate shear strength prediction in this rang of effective stress (*c*'=25 kPa rather than zero in CSE model). Applying the linear shear strength envelope in the slope stability equation will produce an over estimate shear strength for effective stress less than 100 kPa, where the shallow slope failures take a place. This is the reason why conventional shear strength theory fails to model shallow slope failures, which happen at low stress levels.

This also has reported by Md.Noor and Hadi (2010) [14], from the back analysis of Antarabangsa (Selangor, Malaysia) slope failure on 6th December 2008. They used two types of shear strength behavior in order to their slope stability back analysis. Linear shear strength envelope [1], in terms of conventional interpretation of shear strength and CSE model in terms of non-linear shear strength behavior at low stress level. They concluded that, considering of CSE model was capable to back analysis the actual shallow slope failure of Antarabangsa slope failure (factor of safety 0.99 in 10 meters depth of infiltration) while it could not achieve by applying the conventional shear strength method (factor of safety 1.10 in 10 meters depth of infiltration).

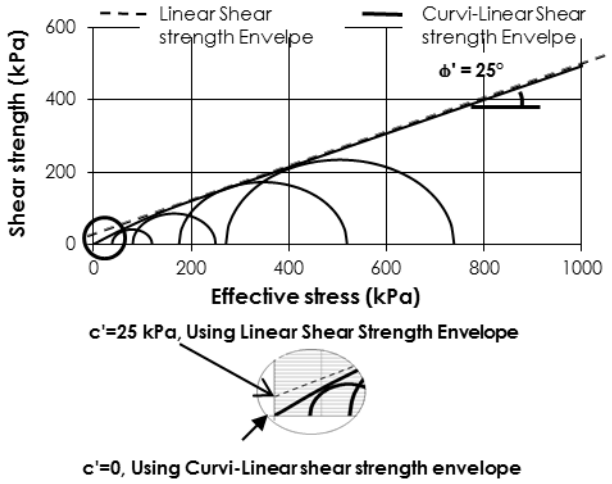


**Figure 5** Mohr circles and linear and curvilinear shear strength envelops from the specimen at fully saturated condition

Table 4, summarizes the shear strength parameters obtained from the Mohr Coulomb envelopes. For all specimens, 200 kPa represents the value of the transition effective stress and the friction angle at failure, $\emptyset_{min\ f}$, is valued at 25 degrees. Apparent cohesion, *c*', is valued at zero for specimens which are saturated and then increases as suction increase. At 6 % moisture content, the optimum value of outward shear strength is reached

(105 kPa) and the value increases. Further, c' drops at 3% moisture content to 35 kPa. The transition shear strength, $\tau_t$, is equal to 120 kPa for saturated specimens. In unsaturated condition, the transition shear strength increases as c' elevates. For example, for 21 kPa of c' in the case of 12 % moisture content, the $\tau_t$ is 141 kPa, whilst as the c' increased to 27 kPa for 9% moisture content, the $\tau_t$ is 147 kPa. The transition shear strength value in unsaturated specimens in specific moisture content is equal to the value of the transition shear strength for saturated condition plus related c'. For example, the value of $\tau_t$ (225 kPa) for 6 % moisture content is equal to the value of $\tau_t$ in a fully saturated condition (120 kPa) plus the value of c' for 6 % moisture content (105 kPa). The comparison of shear strength envelopes for various specimens at saturated and unsaturated conditions is given in Figure 6.

**Table 4** Summary of shear strength parameters obtained for the Mohr Coulomb envelopes

| Soil Specimen Description | $\varphi'_{min\,f}$ | c' (kPa) | $(\sigma - u_w)_f$ (kPa) | $\tau_f$ (kPa) |
|---|---|---|---|---|
| **3% water content (kPa)** | 25 | 35 | 200 | 155 |
| **6% water content (kPa)** | 25 | 105 | 200 | 225 |
| **9% water content (kPa)** | 25 | 27 | 200 | 147 |
| **12% water content (kPa)** | 25 | 21 | 200 | 141 |
| **Fully saturated (kPa)** | 25 | 0 | 200 | 120 |

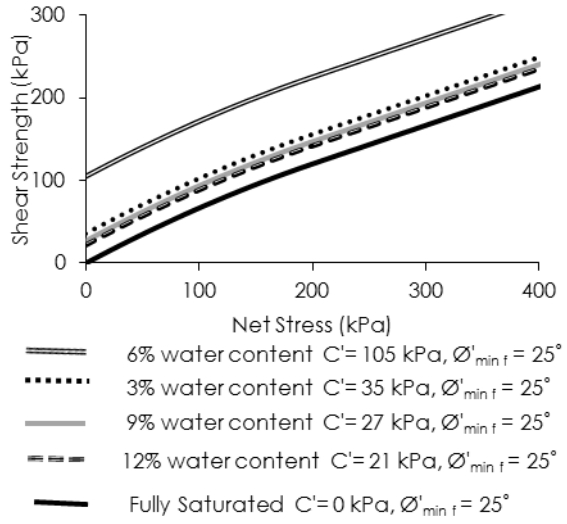


**Figure 6** The comparison of shear strength envelopes for various specimens at saturated and unsaturated conditions

The correlation between apparent cohesion, c', and matric suction at zero net stress is explained in the Curved-Surface envelope soil shear strength model. At zero matric suction (in a fully saturated condition), apparent shear strength is equal to zero in that zone. Further, as matric suction increases, c' also increases sharply. The peak value for c' is reached at residual suction, $(u_a-u_w)_r$. Beyond the maximum c', the graph falls gradually to zero at the ultimate suction at zero net stresses, $(u_a-u_w)_{u^{\sigma'=0}}$.

The aforementioned zone explains the behavior of shear strength with respect to suction. When a suction is equal to residual suction, soil has a maximum value of shear strength [10]. As the soil approaches a saturated condition, shear strength falls steeply. The mentioned behavior is plotted in Figure 7 using Equations 5 and 6.

Based on the CSE model, shear strength behavior with regard to suction is supported by the soli test results (Figure 7). In a specimen with 3 % moisture content, the c' is 35 kPa. It attains to 105 kPa as moisture content hikes up to 6 %. This is almost the same as the moisture content of residual moisture content (8 %). At the increase of moisture content to 9 % and 12 %, there is a sudden decrease in shear strength from 105 kPa to 27 kPa and 21 kPa, respectively. It is a consequent of the mentioned behavior of soil as the soil approaches the saturated condition. At a fully saturated condition, the value of c' finally becomes zero

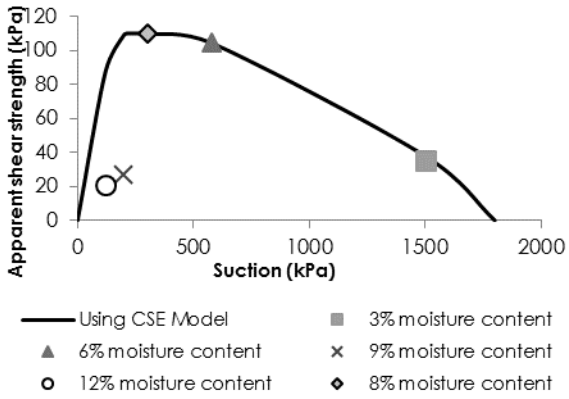


**Figure 7** Shear strength with regard to suction

## 4.0 CONCLUSION

Experimental studies were done on the Malaysian granitic residual soil (grade VI) by conducting the Non-Axis Translation Consolidated Drained Multistage Triaxial test and Pressure Plate Extractor test to characterize the non-linear shear strength behavior of soil tested over an entire range of net stresses and suction range.

The following conclusions can be considered from the study:

1- In each specimen and sample, where they were all under the same consistent effective stress, there is a reduction of the maximum deviator stress from unsaturated specimens to saturated specimens. However, such reduction was also observed from 6% moisture content to 3% moisture content.

2- Curvi-linear Mohr Coulomb envelopes for soil specimens indicates that shear strength in constant suction behaves linearly at high stresses but there is a sudden and a non-linear reduction in shear strength at low effective stress levels (less than 100 kPa).

3- As far as shear strength and its' correlation to suction is concerned, a non-linear behavior is observed. There are two declines in shear strength due to suction: (a) when suction approaches zero and the soil becomes saturated (in 9% and 12% moisture content), (b) when suction is more than residual suction (8% moisture content).

## Acknowledgement

The authors express their sincere gratitude for the support they received from Universiti Teknologi MARA (UiTM).

## References

[1] Terzaghi, K. v. 1936. The Shearing Resistance Of Saturated Soils And The Angle Between The Planes Of Shear. *Proceedings Of The 1st International Conference On Soil Mechanics And Foundation Engineering*. Harvard University Press Cambridge, MA.

[2] Fredlund, D. G., Vanapalli, S. K., Xing, A. and Pufahl, D. E. 1995. Predicting The Shear Strength Function For Unsaturated Soils Using The Soil-Water Characteristic Curve. *First International Conference on Unsaturated Soils.* Paris, France. 6-8.

[3] Fredlund, D. G., Morgenstern, N. R. and Widger, R. A. 1978. The Shear Strength Of Unsaturated Soils. *Canadian Geotechnical Journal.* 15(3): 313-321. doi:10.1139/t78-029.

[4] Charles, J. A. and Watts, K. S. 1980. The Influence Of Confining Pressure On The Shear Strength Of Compacted Rockfill. *Geotechnique*. 30(4): 353-367. doi: 10.1680/geot.1980.30.4.353.

[5] Bishop, A. W. 1966. The Strength Of Soils As Engineering Materials. *Geotechnique*. doi: 10.1680/geot.1966.16.2.91.

[6] Fukushima, S. and Tatsuoka, F. 1984. Strength And Deformation Characteristics Of Saturated Sand At Extremely Low Pressures. *Soils And Foundations.* 24(4): 30-48. http://doi.org/10.3208/sandf1972.24.4_30.

[7] Indraratna, B., L. Wijewardena, and A. Balasubramaniam. 1993. Large-scale Triaxial Testing Of Greywacke Rockfill. *Geotechnique*. 43(1): 37-51. http://dx.doi.org/10.1680/geot.1994.44.3.539.

[8] Rahardjo, H., Lim, T. T., Chang, M. F. and Fredlund, D. G. 1995. Shear-Strength Characteristics Of A Residual Soil. *Canadian Geotechnical Journal*. 32(1): 60-77. http://dx.doi.org/10.1139/t95-005.

[9] Md. Noor, M. J. and M. Hafez 2008. Effective Stress and Complex Soil Settlement Behavior. *EJGE*. 13.

[10] Md. Noor, M. J. and W. Anderson. 2006. A Comprehensive Shear Strength Model For Saturated And Unsaturated Soils. *In Unsaturated Soils 2006. ASCE*.

[11] Escario, V. and J. Saez. 1986. The Shear Strength Of Partly Saturated Soils. *Geotechnique*. 36(3). http://dx.doi.org/10.1680/geot.1986.36.3.453.

[12] Rassam, D. W. and D. J. Williams. 1999. A Relationship Describing The Shear Strength Of Unsaturated Soils. *Canadian Geotechnical Journal.* 36(2): 363-368. http://dx.doi.org/10.1139/t98-102.

[13] Toll, D. G., Ong, B. H., Rahardjo, H. and Leong, E. C. 2000. Triaxial Testing Of Unsaturated Samples Of Undisturbed Residual Soil From Singapore. *In Unsaturated Soils for Asia. Proceedings of the Asian Conference on Unsaturated Soils, UNSAT-Asia*. Singapore, 18-19 May, 2000. AA Balkema. 581-586.

[14] Md. Noor, M. J. and B. Hadi. 2010. The Role Of Curved-Surface Envelope Mohr-Coulomb Model In Governing Shallow Infiltration Induced Slope Failure. *EJGE.* 15.

[15] Kim, J., Jeong, S., Park, S. and Sharma, J. 2004. Influence Of Rainfall-Induced Wetting On The Stability Of Slopes In Weathered Soils. *Engineering Geology*. 75(3): 251-262. http://dx.doi.org/10.1016/j.enggeo.2004.06.017.

[16] Jiang, J.-C., R. Baker, and T. Yamagami. 2003. The Effect Of Strength Envelope Nonlinearity On Slope Stability Computations. *Canadian Geotechnical Journal*. 40(2): 308-325. http://dx.doi.org/10.1139/t02-111.

[17] Lee, I.-M., S.-G. Sung, and G.-C. Cho. 2005. Effect Of Stress State On The Unsaturated Shear Strength Of A Weathered Granite. *Canadian Geotechnical Journal*. 42(2): 624-631. http://dx.doi.org/10.1139/t04-091.

[18] Rassam, D. W. and C. Freeman. 2002. Predicting The Shear Strength Envelope Of Unsaturated Soils. *Geotechnical Testing Journal.* 215-220. http://dx.doi.org/10.1520/gtj11365j.

[19] Vanapalli, S. K., Fredlund, D. G., Pufahl, D. E. and Clifton, A. W. 1996. Model For The Prediction Of Shear Strength With Respect To Soil Suction. *Canadian Geotechnical Journal*. 33(3): 379-392. http://dx.doi.org/10.1139/t96-060.

[20] Guan, G. S., H. Rahardjo, and L. E. Choon. 2009. Shear Strength Equations For Unsaturated Soil Under Drying And Wetting. *Journal Of Geotechnical And Geoenvironmental Engineering*. 136(4): 594-606. http://dx.doi.org/10.1061/(asce)gt.1943-5606.0000261.

[21] Gan, J. K. and D. Fredlund. 1996. Shear Strength Characteristics Of Two Saprolitic Soils. *Canadian Geotechnical Journal*. 33(4): 595-609. http://dx.doi.org/10.1139/t96-085-307.

[22] Kang, J. B., Shin, B. W., Bang, S. T. and Lee, J. D. 2002. Soil-Water Characteristics of Unsaturated Organic Silty Soils. *The Twelfth International Offshore and Polar Engineering Conference. International Society of Offshore and Polar Engineers.*

[23] Fredlund, D. G. and A. Xing. 1994. Equations For The Soil-Water Characteristic Curve. *Canadian Geotechnical Journal*. 31(4): 521-532. http://dx.doi.org/10.1139/t94-120.